IOPscience iopscience.iop.org

Home Search Collections Journals About Contact us My IOPscience

Epitaxial samarium disilicide films on silicon (0 0 1) substrates: growth, structural and electrical properties

This article has been downloaded from IOPscience. Please scroll down to see the full text article.

2011 J. Phys. D: Appl. Phys. 44 135404

(http://iopscience.iop.org/0022-3727/44/13/135404)

View the table of contents for this issue, or go to the journal homepage for more

Download details:
IP Address: 130.195.160.67
The article was downloaded on 16/03/2011 at 20:50

Please note that terms and conditions apply.

J. Phys. D: Appl. Phys. **44** (2011) 135404 (7pp) doi:10.1088/0022-3727/44/13/135404

Epitaxial samarium disilicide films on silicon (0 0 1) substrates: growth, structural and electrical properties

F Natali[1], N O V Plank[1], J Stephen[1,3], M Azeem[1], H J Trodahl[1], B J Ruck[1] and L Hirsch[2]

[1] MacDiarmid Institute for Advanced Materials and Nanotechnology, School of Chemical and Physical Sciences, Victoria University of Wellington, PO Box 600, Wellington 6140, New Zealand
[2] Université de Bordeaux I, IMS Laboratory, CNRS UMR 5218, 16 Av. Pey Berland, 33607 Pessac, France
[3] Industrial Research Limited, P.O.Box 31310, Lower Hutt 5040, New Zealand

E-mail: franck.natali@vuw.ac.nz

Received 4 November 2010, in final form 19 January 2011
Published 16 March 2011
Online at stacks.iop.org/JPhysD/44/135404

Abstract
In this paper the effect of the growth temperature on the structural and electrical properties of samarium silicide films is investigated. The growth of the epitaxial films is performed under ultrahigh vacuum by reactive-deposition epitaxy on silicon (0 0 1) substrates. The structural properties are assessed by reflection high-energy electron diffraction and x-ray diffractometry. Random and channelling Rutherford backscattering experiments show that the films have the correct stoichiometry, i.e. Sm/Si ratio = 1 : 2, with channelling yields as low as 20% for the best samples. The electrical properties of these films are studied by Hall effect and resistivity measurements. The films have a metallic character, with a high concentration of n-type charge carriers ($>10^{22}$ cm^{-3}) and a resistivity lower than 200 $\mu\Omega$ cm at room temperature. The metallic character is confirmed by the experimental optical conductivity deduced from ellipsometry experiments. Finally, evidence is presented showing the potential of $SmSi_2$/n-type Si junctions for electronic application with a Schottky barrier height of about 0.32 eV.

(Some figures in this article are in colour only in the electronic version)

1. Introduction

The continuous reduction in the complementary metal–oxide–semiconductor (CMOS) dimensions towards tenths of nanometres or less presents severe materials and processing challenges. Among the most critical problems are the satisfactory formation of interconnects, contacts and the source/drain (S/D) area [1–3]. For the latter, it has been proposed to replace the highly doped silicon S/Ds by metallic S/Ds in order to reduce the impact of their series resistances on transistor performance [4, 5]. In that context, the potential of rare-earth silicide (RESi) films has sparked renewed interest due to their low Schottky barrier heights (SBH): (∼0.3–0.4 eV) and (∼0.7–0.8 eV) on n-type and p-type silicon, respectively [6–9]. They are thus ideal candidates for infrared detectors, metal base transistors, rectifier diodes as well as high speed switching and radio-frequency applications. Furthermore they have a relatively low resistivity [8, 10], a low lattice mismatch with Si(1 1 1) [11] and the possibility of epitaxial growth [11]. Although it is still unclear if epitaxial layers are superior to polycrystalline layers, the advantages of epitaxial over polycrystalline silicides could be numerous at the nanometre scale: a better control and improvement of the metal/semiconductor interfaces will provide a low specific contact resistance [12, 13] and the absence of grain boundaries would decrease electromigration-related problems [14].

Most of the studies of RESi were performed in the 1980s and onto (1 1 1) oriented silicon substrates [11, 15]. In that configuration most of the rare earths form a Si-rich silicide phase ($RESi_{\sim 1.7}$) with the hexagonal AlB_2 type structure which grows epitaxially relatively easily on the (1 1 1) surface of Si [11, 16]. However, with the aim of integrating RESi into silicon-based microelectronics, the Si(0 0 1) substrate is preferred as it is the most widely used in the silicon mainstream

 © 2011 IOP Publishing Ltd Printed in the UK & the USA

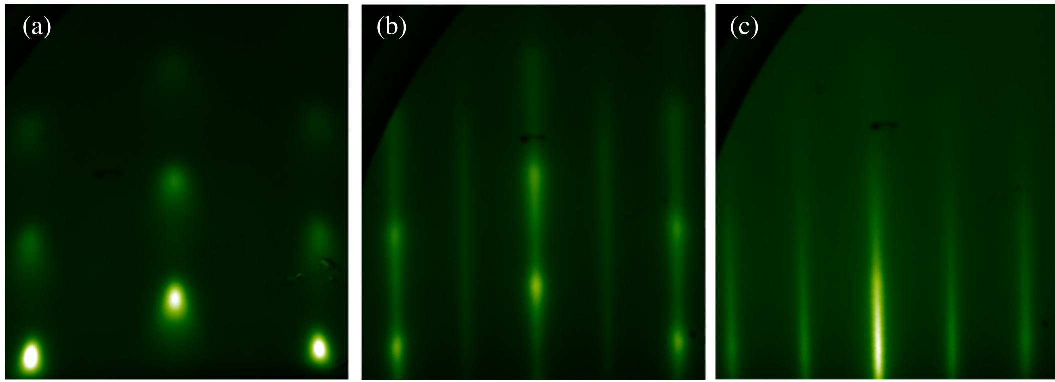

Figure 1. RHEED pattern along the Si[1 1 0] azimuth of a 40 nm thick $SmSi_2$ layer grown at (*a*) 375 °C, (*b*) 500 °C and (*c*) 600 °C. The images are taken at room temperature.

technology. Little attention has been dedicated to the growth of thin RESi layers on this face mainly due to a severe lattice mismatch. However the few results available demonstrate that $ErSi_{1.7}$ [17–19], $DySi_{1.7}$ [20], $GdSi_2$ [21] and $LuSi_{1.7}$ [22] can be grown epitaxially onto (0 0 1) oriented silicon surfaces. Recently, we have expanded this set by growing epitaxially $SmSi_2$ films on Si(0 0 1) [23]. In this work we explore the effect of the growth temperature on the structural, electrical and optical properties of epitaxial $SmSi_2$ thin films grown by reactive-deposition epitaxy (RDE) on Si(0 0 1). We have also grown and characterized polycrystalline films prepared by the solid phase reaction (SPR) technique which is the most common growth technique used for silicide thin films, and have compared their properties with epitaxial films. The aim of this work is to study growth conditions and properties of thin films of Sm silicide grown on Si and evaluate their applicability in the Si microelectronic technology. Finally, we extract temperature-dependent SBHs for $SmSi_2$/n-type Si(0 0 1) contacts from current–voltage measurements to assess their potential use metallic source/drain in Schottky barrier MOS technology.

2. Experiments

Our experiments have been performed on highly resistive (>1000 Ω cm) and n-type (5–10 Ω cm) Si(0 0 1)-oriented substrates in a thermionics ultrahigh vacuum (UHV) system. Sm metal is evaporated either from a tungsten wire basket or using an electron beam. The evaporation system is equipped with a turbopump which gives a base pressure $<10^{-8}$ Torr and about 5×10^{-8} Torr during evaporation of Sm. Prior to the growth, substrates are first thermally outgassed at ∼600 °C for 2 h, and then the native oxide is removed by rapid thermal annealing at 950 °C. The appearance of the (2 × 2) surface reconstruction, followed by reflection high energy electron diffraction (RHEED) along the [1 1 0] Si azimuth, indicated that the surface was clean and well ordered.

We grew samarium silicide films by RDE, evaporating samarium onto hot silicon substrates at different temperatures. To compare the effect of the growth temperature on the properties of the $SmSi_2$ layers, we rapidly decrease the sample temperature as soon as the growth is completed to prevent further interdiffusion and smoothing. As a consequence the RHEED patterns presented below were taken at room temperature. The evaporation rate is measured by a quartz-crystal thickness monitor. The stoichiometry, the layer thickness and degree of crystallinity of the samarium silicide layers were determined by random and channelling Rutherford backscattering spectroscopy (RBS) experiments using a 2 MeV $^4He^+$ ion beam. The structural properties of the layers were investigated by x-ray diffraction (XRD) measurements using Cu-Kα radiation. Electron transport measurements have been carried out using a van der Pauw configuration and the optical conductivity was measured by ellipsometry using a Beaglehole Instruments Picometer. The SBH was determined using the activation-energy-based method [9, 24] on structures consisting of two silicided contacts separated by a bare-Si gap.

3. Growth and structural properties of samarium disilicide layers

Our first goal was to study the effect of the growth temperature (T_g) on the growth mode of the $SmSi_2$ layer using RHEED analysis. For growth temperature below ∼300–350 °C, the RHEED pattern results in a diffuse halo which is composed, after a few nanometres, of well-resolved Debye rings characteristic of a polycrystalline layer. The RHEED pattern was observed to be independent of the azimuthal incidence of the electron beam which suggests random orientation of the crystal grains in azimuthal planes. XRD 2θ-scan performed on these samples show both the presence of polycrystalline $SmSi_2$ and lines that we attributed to some unreacted Sm metal. When the Sm impinges onto the Si surface above a temperature of 300–350 °C, we observe a change in the diffraction pattern from polycrystalline to spotty, corresponding to a three-dimensional growth mode, as shown in figure 1(*a*). By increasing the growth temperature, the shape of the diffraction pattern becomes sharper and more intense; from modulated at 500 °C (figure 1(*b*)) and then streaky, indicating a very smooth, flat growing surface, at even higher temperature (figure 1(*c*) for $T_g = 650$ °C). Upon further growth at 600–650 °C to increase the thickness, the RHEED pattern results in sharper and more intense diffraction streaks [23]. This phenomenon is not observed for layers

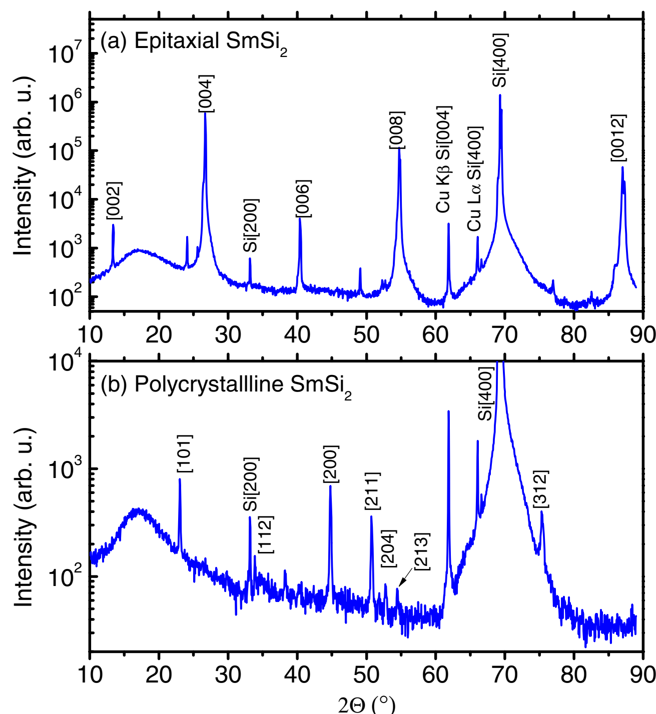

Figure 2. Typical XRD 2Θ-scan of (*a*) an epitaxial $SmSi_2$ layer grown by RDE and (*b*) a polycrystalline $SmSi_2$ layer grown by the solid phase transition on (0 0 1) oriented substrates.

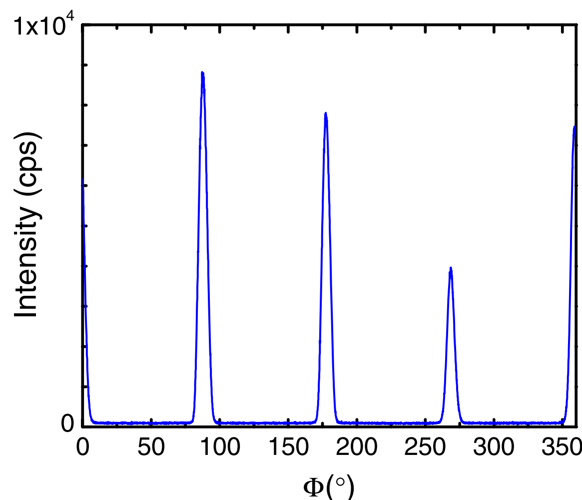

Figure 3. Typical XRD Φ-scan of the (0 0 1) $SmSi_2$ plane indicating a 4-fold symmetry.

grown at 375 and 500 °C. A Sm deposition rate ranging from 0.1 to 0.5 nm s^{-1} does not affect the growth mode and the structural properties. RHEED analysis shows that the unit cell of the $SmSi_2$ crystal is rotated 45° with respect to that of the Si unit cell, $SmSi_2$[1 0 0] ∥ Si[1 1 0], in order to reduce the lattice mismatch from +25.6% to −5.2% [23]. The in-plane lattice parameter deduced from the RHEED pattern of the film along the Si [1 1 0] azimuth is 4.03 Å, in agreement with the value observed in the tetragonal bulk structure of $SmSi_2$ (4.041 Å) [25]. We also observe a (2 × 2) surface reconstruction on the RHEED patterns, whose intensity progressively vanishes when the $SmSi_2$ surface becomes more and more rough, from the 2D to 3D character of the surface. Further details about this surface reconstruction can be found elsewhere (see [23]).

XRD 2θ-scans were performed on samples grown at 375, 500 and 650 °C. In all cases we see only the lines corresponding to the (0 0 1) family of $SmSi_2$ planes showing a preferred orientation of the silicide layers relative to the silicon substrate with their *c*-axis lying in the (0 0 1) Si planes. Figure 2(*a*) displays the typical XRD 2θ-scan of epitaxial layers. Upon increasing the growth temperature we observe a significant reduction in the linewidth of the [0 0 4] peak from 0.511°, 0.3532° to 0.255° for temperatures of 375 °C, 500 °C and 650 °C, respectively. An increase in the growth temperature is clearly helpful for achieving a higher crystal quality of the $SmSi_2$ layer. The implied lattice constant along the growth axis is found to be 13.32 Å, in agreement with the expected bulk value of 13.3 Å [25]. It has been reported in the literature that a phase transition from orthorhombic to tetragonal occurs for $SmSi_2$ as the temperature is raised past 380 °C [26, 27]. In our films we see no evidence for such a phase transition. The difference between the in-plane lattice constants in the two phases is slight, and the contrast between the *a*- and *b*-axis of the orthorhombic phase is very small, approximately 1% [25]. In particular, an XRD Φ-scan of the (0 0 1) $SmSi_2$ plane (figure 3) indicates a 4-fold symmetry but the peak intensity does not allow any conclusions concerning the orthorhombic or tetragonal phase at room temperature.

It is important to point out that the deposition of Sm directly onto the native oxide (SiO_2) on the silicon substrate at 600 °C also leads to the formation of samarium disilicides. The structural properties of such films do not differ to the one presented in this work. Such results have already been reported for thin rare-earth-metal overlayers (Pr, Eu, Gd and Yb) by Hoffman *et al* [28]. They showed that a chemical reaction between the SiO_2 and the rare-earth metal atoms yields metal silicide and metal oxide, thereby reducing the SiO_2.

As a comparison we have also grown thin films using the SPR technique, which is a well-known growth technique used for silicide thin films. One evaporates first a samarium layer at room temperature. Annealing, under UHV, the RE–Si interface promotes RE and Si interdiffusion which induces the formation of various silicide compounds. In our case, as soon as the growth starts, the RHEED pattern presents a diffuse halo which is composed, after a few nanometres, of well-resolved Debye rings characteristic of a polycrystalline layer. The sample was annealed *in-situ* to form the silicides at a temperature of 650 °C for 30 min. We observe no modification of the RHEED pattern during annealing. Figure 2(*b*) displays the typical XRD 2θ-scan of polycrystalline layers grown by SPR. We do not see preferred textured direction of the films. Furthermore, we do not observe lines that we could attribute to some unreacted Sm metal. Clearly Sm does not form epitaxial silicide layers when reacted in the solid phase as readily as other RESi. For example, epitaxial $GdSi_2$ on the Si(0 0 1) substrate was observed after annealing at 500 °C for 5 min [29].

To obtain more quantitative information on the epitaxial nature of the grown layer, RBS in random and channelling conditions was undertaken. Figure 4 shows the random and aligned spectra of a 265 nm thick $SmSi_2$ layer grown at

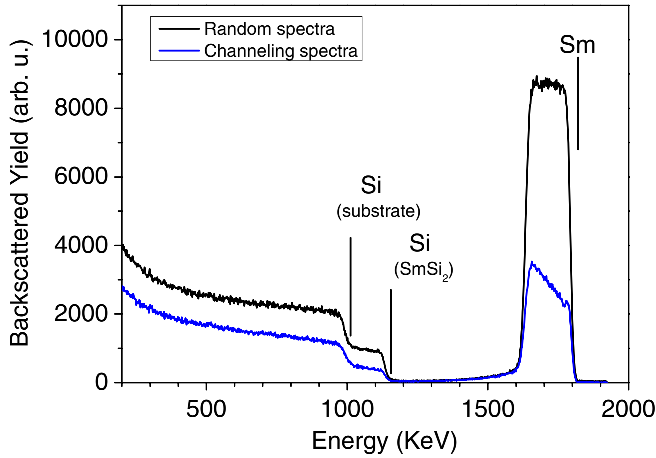

Figure 4. Rutherford backscattering yield in random (blue) and aligned (black) conditions as a function of the energy for a 2 MeV $^4He^+$ ion beam with a 160° scattering angle for a 265 nm thick $SmSi_2$ film. Random spectrum was done with a rotating sample with a 5° tilt angle.

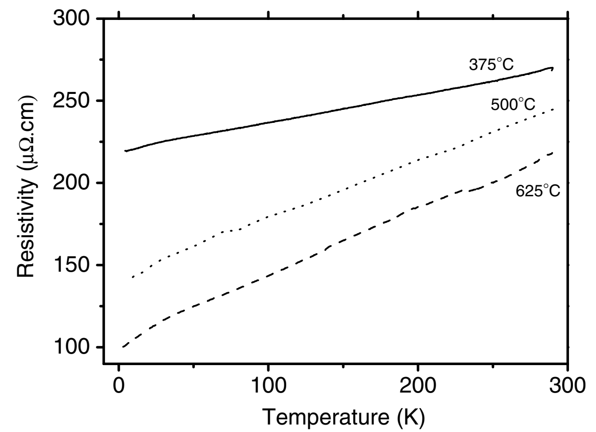

Figure 5. Resistivity as a function of the temperature for 40 nm thick films. The growth temperature is indicated (°C) on the curves.

600–650 °C. The arrows (labelled Sm and Si) indicate the energy for backscattering from these elements at the surface. The random spectrum shows that a continuous $SmSi_2$ layer is formed on these samples. The Sm/Si ratio is measured to be constant throughout the $SmSi_2$ film indicating good film uniformity. It is found to be 1 : 2, independent of film thickness ranging from 40 nm to 1.3 μm, and without the appearance of significant Si vacancies, as is usually observed in the RESi growth. The χ_{min} value, calculated as the ratio near the surface of the backscattering yield under channelling condition to that for a random beam incidence, obtained from the Sm part is equal to 26.5% and 20% ± 0.5% for a 265 nm and 1.3 μm thick $SmSi_2$ layers, respectively. Note that no reliable value can be calculated for 40 nm thick $SmSi_2$ layers. In spite of the large lattice mismatch between the silicon (0 0 1) substrate and the $SmSi_2$ layer, this value is comparable to the best RESi layers grown on a nearly lattice-matched silicon (1 1 1) substrate. Indeed, values of χ_{min} about 20%, 26% and 10% have been reported for $ErSi_{1.7}$ [30], $YSi_{1.7}$ [11], and $GdSi_{1.7}$ [31], respectively.

4. Electrical measurements and Schottky barrier

4.1. Resistivity and Hall effect

$SmSi_2$ films from 250 nm to 1.3 μm thick grown at 600–650 °C showed a temperature-dependent resistivity typical of a metal [23]. The residual resistivity $\rho_{4\,K} = 80\,\mu\Omega$ cm is comparable to the intrinsic phonon-limited resistivity $\rho_{in} = \rho_{300\,K} - \rho_{4\,K} = 90\,\mu\Omega$ cm, indicating a moderate level of disorder scattering [23]. There is no evidence of an anomaly that might signal a magnetic ordering temperature as has been reported for $ErSi_2$ [8], $GdSi_{1.7}$ [10] or $DySi_{2-x}$ [18]. However, for 40 nm thick films, a weak anomaly is observed below 50 K, and the resistivity does not saturate to a low temperature limit resistivity (figure 5). A full discussion of this phenomenon is beyond the scope of this paper and needs further investigations. Both the intrinsic resistivity and ambient-temperature resistivity of films are somewhat larger than found for $ErSi_{1-x}$ [8, 10], $GdSi_{1-x}$ [10, 32] and $DySi_{2-x}$ [20], but comparable to most other RESis [20, 22, 33]. By decreasing the thickness of the $SmSi_2$ films towards 40 nm there is a moderate increase in the resistivity, $\rho_{4\,K} = 100\,\mu\Omega$ cm still comparable to the intrinsic phonon-limited resistivity $\rho_{in} = \rho_{300\,K} - \rho_{4\,K} = 116\,\mu\Omega$ cm (figure 5). Such a resistivity is still too high to propose $SmSi_2$ as an alternative material to replace Cu as interconnect. However, we may expect to reduce its resistivity by codeposition of Sm and Si in the atomic ratio 1 : 2 and/or annealing process, as observed for ErSi or FeSi systems. Resistivities of 40 nm thick $SmSi_2$ films grown at 375 and 500 °C are also reported in figure 5. The behaviour of the resistivity as a function of the temperature of these two is a typically metallic one.

We observe that a decrease in the growth temperature results in an increase in the film resistivity both for $\rho_{300\,K}$ and $\rho_{4\,K}$, which correlates well with the crystalline quality of the films as measured by XRD. The increased resistivity is especially strong for the film grown at 375 °C, which is very close to the transition between the low-temperature orthorhombic phase and the high temperature tetragonal phase of $SmSi_2$, 380 °C. A mixture of different phases is known to increase significantly the resistivity in the silicide-based compounds [34].

The Hall coefficient is found to be negative at all temperatures, i.e. the predominant free carriers are electrons. Its magnitude is a slightly decreasing function of the temperature from about 7.5×10^{-4} cm^3 C^{-1} at 4 K to about 6×10^{-4} cm^3 C^{-1} at room temperature (figure 6). The room temperature value corresponds to a carrier concentration of about 1.1×10^{22} cm^{-3}, about a factor of two larger than found in other RESis. The carrier concentration is very similar to those reported for transition metal silicides such as CoSi [35], WSi [36] or NiSi [35] where the free carriers are predominantly holes. These are all characteristic of approximately half-filled bands and complex Fermi surfaces. In that case the Hall coefficient depends on the variation of the velocity, effective mass tensor and relaxation time around the Fermi surface, and yields a merely approximate value for the carrier concentration [37]. The temperature dependence of the Hall coefficient does

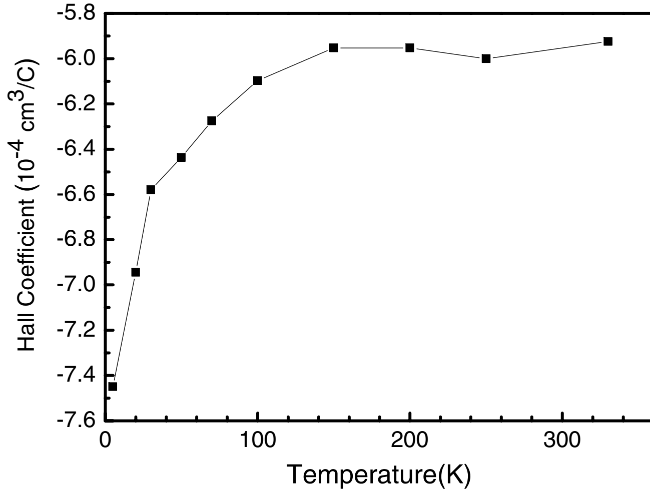

Figure 6. Hall coefficient as a function of the temperature for a 490 nm thick $SmSi_2$ films.

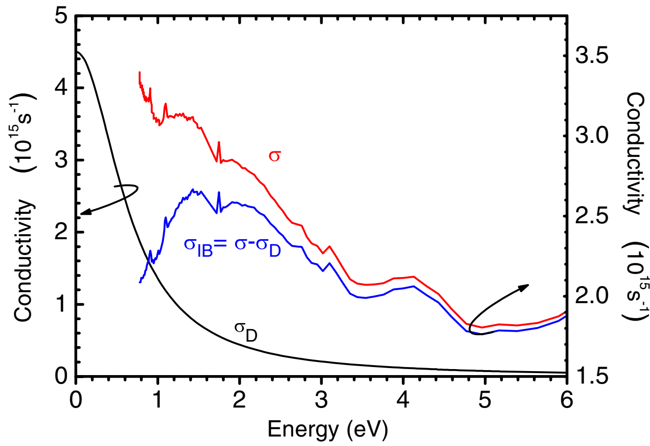

Figure 7. Experimental optical conductivity (σ), with a separation into the free-carrier (σ_D) and inter-band (σ_{IB}) contributions, at room temperature.

not then signal a temperature-dependent carrier concentration. Indeed such a temperature-dependent Hall coefficient has been known in, for example, Cu for at least a century [38, 39]. The metallic nature of the films is further demonstrated by the experimental optical conductivity (σ at room temperature shown in figure 7, with a separation into the free-carrier (σ_D) and inter-band (σ_{IB}) contributions. The latter shows clear transitions near 1.4 and 4.0 eV. The calculated free-carrier (Drude) contribution to the optical conductivity is given by $\sigma_D = \sigma(0)/(1 + \omega^2\tau^2)$, where $\tau \approx 1.7 \times 10^{-15}$ s^{-1} for $n \approx 1.05 \times 10^{22}$ cm^{-3} is determined by the dc conductivity and Hall effect. That free-carrier conductivity is shown, along with the inter-band conductivity, $\sigma_{IB} = \sigma - \sigma_D$. There are as yet no theoretical band structure results for $SmSi_2$ to which these inter-band transitions can be compared. The bands in $ErSi_2$, for which a calculation is available, show ample structure for inter-band transitions in the 1–6 eV range [40].

Finally, we state that polycrystalline thin films present a higher resistivity than epitaxial thin films; typical values for the former are about 5800 $\mu\Omega$ cm at RT and 4700 $\mu\Omega$ cm at 4 K. Thus as expected the mean free path of the charge carriers is larger in epitaxial films than in polycrystalline films.

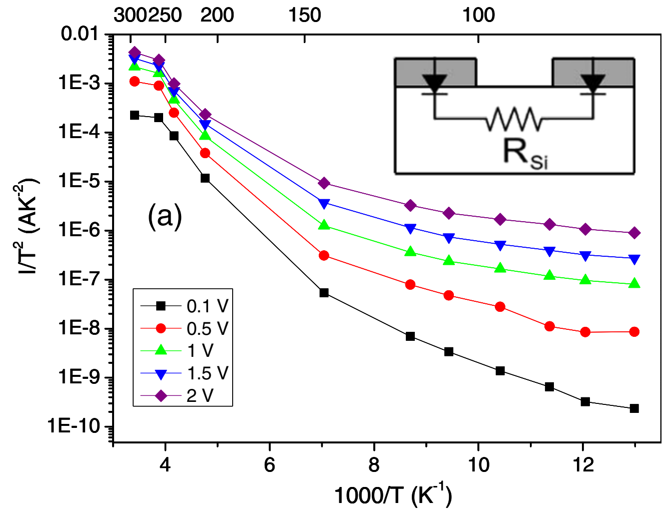

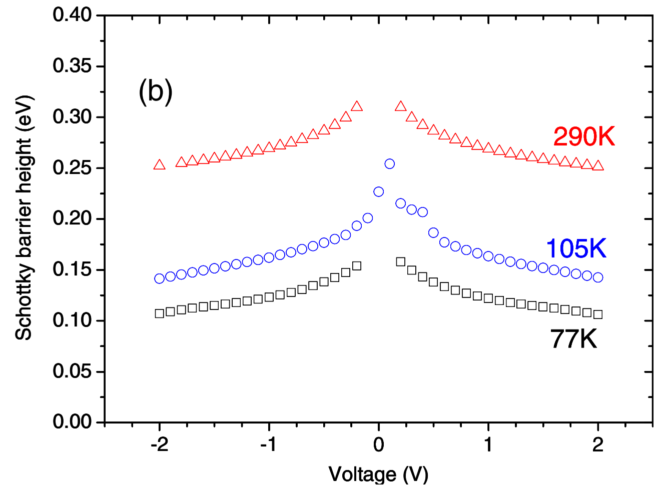

Figure 8. (*a*) Arrhenius plots of two back to back $SmSi_2$/n-type Si Schottky junctions for various voltages, (*b*) voltage dependence of the effective Schottky barrier to electrons measured on $SmSi_2$–Si Schottky junctions for temperature of 290, 105 and 77 K.

4.2. Schottky barrier height

In order to extract the SBH we have used the activation-energy-based method consisting of two silicided contacts separated by a bare-Si gap. This structure (see the inset to figure 8(*a*)), as mentioned by Reckinger *et al* ([9]), simulates the source/channel/drain of a real Schottky barrier MOSFET (SB-MOSFET). The $SmSi_2$ layer was grown at 600 °C on a n-type (5–10 Ω cm) (0 0 1) silicon substrate and the face-to-face Schottky diodes were defined by lithography and by wet etching using a solution of HCl. Using this geometry, the reverse current I_R flowing in one of the junctions can be described by the thermionic emission model in the following form $\ln(I_R/T^2) = \ln(SA^*) - (q/kT)\Phi_{beff}$ where Φ_{beff} is the Schottky barrier, A^* the effective Richardson constant and S the surface of the junction. The gap between the $SmSi_2$/Si contacts is about 500 μm while the junction area is about 1 × 1 mm^2. Current versus voltage curves of face-to-face Schottky diodes were obtained by two-contact measurements at temperature ranging from 290 to 77 K. Then, the curves were converted into Arrhenius plots for some selected bias as shown in figure 8(*a*) in order to extract the SBH. The

non-linear Arrhenius plot suggests that the effective barrier height for electrons varies with temperature, which is usually due to the imperfection of the Schottky junction such as spatially inhomogeneous barrier or interface states [41, 42]. It is important to note also that the change in the slope at RT might be due to a contribution of the silicon substrate series resistance. Figure 8(*b*) shows the extracted barrier height as a function of the applied voltage for temperature of 290, 105 and 77 K. The barrier height near zero voltage is found to be about 0.15 eV at 77 K and about 0.32 eV at room temperature. The variation of the SBH as a function of the applied voltage for a given temperature is caused by the deviation of the thermionic model used. This is expected to be due to complex combination of the thermionic, field emission and tunnelling transport mechanisms as well as the barrier lowering effect [43]. These values are comparable to those of other RESis on n-type Si, both (1 1 1) and (0 0 1) orientation [4–6, 21, 22]. To the best of our knowledge, no Schottky barrier characteristics of $SmSi_2$/Si contacts have been reported up to now.

5. Conclusion

In summary, we have investigated the RDE of samarium silicide films on silicon (0 0 1). The effect of the growth temperature on the structural and electrical properties is reviewed. The tetragonal films are grown with a preferred matching face relationship on (0 0 1) silicon, $SmSi_2$[1 0 0] ∥ Si[1 1 0]. We show that an increase in the growth temperature up to 600–650 °C is clearly helpful for achieving a higher crystal quality of the thin films. We also demonstrate using RBS that the films grow with the correct stoichiometry such that the Sm to Si ratio is 1 : 2 with a good epitaxial quality. The thin films have a metallic character, confirmed by optical measurements, with a low resistivity and a high n-type carrier concentration. Finally we measured a SBH on n-type Si of 0.32 eV at room temperature. These results are promising for applications in silicon-based electronics.

Acknowledgments

The authors are grateful to A Hyndman, G V M Williams and M Ryan for rocking curve and phi-scan measurements. One of the authors (FN) wants to thank the CENBG (France) for providing access to AIFIRA (Application Interdisciplinaire des Faisceaux d'Ions en Aquitaine) facility. The research reported here was supported by a grant from the New Economy Research Fund (contract VICX0808).

References

[1] Larson J M and Snyder J P 2006 *IEEE Trans. Electron Devices* **53** 1048
[2] Leong M, Narayanan M I, Singh D, Topol A, Chan V and Ren Z 2006 *Mater. Today* **9** 26
[3] Connelly D, Faulkner C and Grupp D E 2003 *IEEE Trans. Electron Devices* **50** 1340
[4] Noori A M *et al* 2008 *IEEE Trans. Electron Devices* **55** 1259
[5] Ostling M, Gudmundsson V, Hellstrom PE, Malm B G, Zhang Z and Zhang S L 2008 *9th Int. Conf. on Solid-State and Integrated-Circuit Technology (Beijing)* vols 1–4, p 146
[6] Tu K N, Thompson R D and Tsaur B Y 1981 *Appl. Phys. Lett.* **38** 626
[7] Norde H, de Sousa Pires J, d'Heurle F, Pesavento F, Petersson S and Tove P A 1981 *Appl. Phys. Lett.* **38** 865
[8] Duboz J Y, Badoz P A, Arnaud d'Avitaya F and Chroboczek J A 1989 *Appl. Phys. Lett.* **55** 84
[9] Reckinger N *et al* 2009 *Appl. Phys. Lett.* **94** 191913
[10] Hogg S M, Vantomme A and Wu M F 2002 *J. Appl. Phys.* **91** 3664
[11] Knapp J A and Picraux S T 1986 *Appl. Phys. Lett.* **48** 466
[12] Massies J, Chaplart J, Laviron M and Linh N T 1981 *Appl. Phys. Lett.* **38** 693
[13] Missous M, Rhoderick E H and Singer K E 1986 *J. Appl. Phys.* **59** 3189
Missous M, Rhoderick E H and Singer K E 1986 *J. Appl. Phys.* **60** 2439
[14] Zhigal'skii G P and Jones B K 2003 *The Physical Properties of Thin Metal Films* (*Electrocomponent Science Monographs*) (Boca Raton, FL: CRC press)
[15] Baglin J E E, d'Heurle F M and Petersson C S 1981 *J. Appl. Phys.* **52** 2841
[16] Vandré S, Kalka T, Preinesberger C and Dähne-Prietsch M 1999 *Phys. Rev. Lett.* **82** 1927
[17] Lee Y K, Fujimura N, Ito T and Itoh N 1993 *J. Cryst. Growth* **134** 247
[18] Travlos A, Salamouras N and Flouda E 1997 *Appl. Surf. Sci.* **120** 355
[19] Frangis N, Van Landuyt J, Kaltsas G, Travlos A and Nassiopoulos A G 1997 *J. Cryst. Growth* **172** 175
[20] Travlos A, Salamouras N and Boukos N 2001 *Thin Solid Films* **397** 138
[21] Gerőcs I, Molnár G, Jároli E, Zsoldos E, Petö G, Gyulai J and Bugiel E 1987 *Appl. Phys. Lett.* **51** 2144
[22] Travlos A, Aloupogiannis P, Rokofyllou E, Papastaïkoudis C, Weber G and Traverse A 1992 *J. Appl. Phys.* **72** 948
[23] Natali F, Plank N O V, Ludbrook B M, Richter J, Minnee T, Ruck B J, Trodahl H J, Kennedy J V and Hirsch L 2010 *Japan. J. Appl. Phys.* **49** 025505
[24] Dubois E and Larrieu G 2004 *J. Appl. Phys.* **96** 729
[25] Morozkn A V, Seropegin Y D, Sviridov I A, Moskalev V A, Tskhadadze I A and Ryabinkin I G 1998 *J. Alloys Compounds.* **280** 178
[26] Gokhale A B and Abbaschian G J 1988 *Bull. Alloy Phase Diagr.* **9** 582
[27] Gorbachuk N P and Bolgar A S 2000 *Powder Metall. Met. Cera.* **39** 567
[28] Hofmann R, Henle W A, Öfner H, Ramsey M G, Netzer F P, Braun W and Horn K 1993 *Phys. Rev.* B **47** 10407
[29] Molnár G, Gerõcs I, Petõ G, Zsoldos E, Gyulai J and Bugiel E 1991 *Appl. Phys. Lett.* **58** 249
[30] Duboz J-Y, Badoz P-A, Perio A, Oberlin J-C, Arnaud D'Avitaya F, Campidelli Y and Chroboczek J A 1989 *Appl. Surf. Sci.* **38** 171
[31] Wu M F, Vantomme A, Pattyn H, Langouch G and Bender H 1996 *Appl. Phys. Lett.* **68** 3260
[32] Guizzetti G, Mazzega E, Michelini M, Nava F, Borghesi A and Piaggi A 1990 *J. Appl. Phys.* **67** 3393
[33] Pierre J, Siaud E and Frachon D 1988 *J. Less-Common Met.* **139** 321
[34] Gas P, Tardy F J and d'Heurle F M 1987 *J. Appl. Phys.* **61** 193
[35] Hensel J C, Tung R T, Poate J M and Unterwald F C 1984 *Appl. Phys. Lett.* **44** 913
[36] Li B Z and Aitken R G 1985 *Appl. Phys. Lett.* **46** 401
[37] Blatt F J 1968 *Physics of Electronic Conduction in Solids* (New York: McGraw-Hill)

[38] Smith A W 1910 *Phys. Rev. (Series I)* **30** 1
[39] Caton R, Sarachik M P and Bloomfield P E 1974 *Phys. Rev.* B **10** 2987
[40] Allan G, Lefebvre I and Christensen N E 1993 *Phys. Rev.* B **48** 8572
[41] Werner J H and Guttler H H 1991 *J. Appl. Phys.* **69** 1522
[42] Aniltürk Ö S and Turan R 2000 *Solid-State Electron.* **44** 41
[43] Hernández M P, Alonso C F and Pena J L 2001 *J. Phys. D: Appl. Phys.* **34** 1157